


Nitrate isotopes reveal N-cycled waters in a spring-fed agricultural catchment

Ioannis Matiatis, Luis Araguás-Araguás, Leonard I. Wassenaar, Lucilena Rebelo Monteiro, Astrid Harjung, Cedric Douence & Martin Kralik


To cite this article: Ioannis Matiatis, Luis Araguás-Araguás, Leonard I. Wassenaar, Lucilena Rebelo Monteiro, Astrid Harjung, Cedric Douence & Martin Kralik (2023) Nitrate isotopes reveal N-cycled waters in a spring-fed agricultural catchment, *Isotopes in Environmental and Health Studies*, 59:1, 27-47, DOI: [10.1080/10256016.2022.2157412](https://doi.org/10.1080/10256016.2022.2157412)


To link to this article: <https://doi.org/10.1080/10256016.2022.2157412>

 View supplementary material [↗](#)

 Published online: 23 Dec 2022.

 Submit your article to this journal [↗](#)

 Article views: 120

 View related articles [↗](#)

 View Crossmark data [↗](#)



Nitrate isotopes reveal N-cycled waters in a spring-fed agricultural catchment

Ioannis Matiatos^a, Luis Araguás-Araguás^{lb}, Leonard I. Wassenaar^{lb},
Lucilena Rebelo Monteiro^{lb}, Astrid Harjung^b, Cedric Douence^b and Martin Kralik^e

^aHellenic Centre for Marine Research, Institute of Marine Biological Resources and Inland Waters, Anavissos Attikis, Greece; ^bInternational Atomic Energy Agency, Isotope Hydrology Section, Vienna International Centre, Vienna, Austria; ^cWasserCluster Lunz Biological Station, Lunz am See, Austria; ^dInstituto de Pesquisas Energéticas e Nucleares, IPEN/CNEN – Cidade Universitária, São Paulo, Brazil; ^eDivision of Environmental Geosciences (EDGE), Center for Microbiology and Environmental Systems Science (CMES), University of Vienna, Vienna, Austria

ABSTRACT

Nitrate stable isotopes provide information about nitrate contamination and cycling by microbial processes. The Fischadagnitz (Austria) spring and river system in the agricultural catchment of the Vienna basin shows minor annual variance in nitrate concentrations. We measured nitrate isotopes ($\delta^{15}\text{N}$, $\delta^{18}\text{O}$) in the source spring and river up to the confluence with the Danube River (2019–2020) with chemical and water isotopes to assess mixing and nitrate transformation processes. The Fischadagnitz spring showed almost stable nitrate concentration (3.3 ± 1.0 mg/l as $\text{NO}_3\text{-N}$) year-round but surprisingly variable $\delta^{15}\text{N}$, $\delta^{18}\text{O}\text{-NO}_3$ values ranging from +5.5 to +11.1‰ and from +0.5 to +8.1‰, respectively. The higher nitrate isotope values in summer were attributed to release of older denitrified water from the spring whose isotope signal was dampened downstream by mixing. A mixing model suggested denitrified groundwater contributed > 50 % of spring discharge at baseflow conditions. The isotopic composition of NO_3 in the gaining streams was partly controlled by nitrification during autumn and winter months and assimilation during the growing season resulting in low and high $\delta^{15}\text{N}\text{-NO}_3$ values, respectively. NO_3 isotope variation helped disentangle denitrified groundwater inputs and biochemical cycling processes despite minor variation of NO_3 concentration.

ARTICLE HISTORY

Received 24 June 2022
Accepted 9 November 2022


KEYWORDS

Agricultural catchment; biogeochemistry; denitrification; groundwater; isotope hydrology; mixing; nitrogen-15; nitrate; oxygen-18

1. Introduction

Nitrate (NO_3) is one of the most widespread pollutants in rivers and groundwater primarily due to diffuse and point source inputs from agricultural fertilizers and manures, domestic or industrial wastewater effluent discharge and increased atmospheric deposition [1–4]. Excess nitrate can result in eutrophication of rivers and lakes and thereby reduce the

CONTACT Ioannis Matiatos  i.matiatos@hcmr.gr  Hellenic Centre for Marine Research, Institute of Marine Biological Resources and Inland Waters, 46,7 km of Athens-Sounio Ave., 19013, Anavissos Attikis, Greece

 Supplemental data for this article can be accessed online at <https://doi.org/10.1080/10256016.2022.2157412>.

© 2022 Informa UK Limited, trading as Taylor & Francis Group

biodiversity and aquatic ecosystem health. Moreover, high concentrations of nitrate pose risks to human health, e.g. infant methemoglobinemia, human gastric cancer (e.g. [5]), and as a result the World Health Organization (WHO) and many governments set quality standards for water resources, management regulations and guidelines for the use and disposal of water in the consumption sector, including for nitrate [6].

When rainwater infiltrates into the subsurface, it may be stored in the aquifers for many years, but often groundwater discharges onto the surface via springs or as stream baseflow. The fate of nitrate in the unsaturated zone above aquifers is controlled by biogeochemical oxidation and reduction processes, which control the prevalent nitrogen species (e.g. NO_3^- , NH_4^+). In aquifers under aerobic conditions, oxidation of organic carbon is performed by aerobic bacteria, which use dissolved oxygen for oxidation of reduced N forms [7]. After dissolved oxygen is consumed anaerobic bacteria use nitrate as the electron acceptor, resulting in the denitrification of nitrate to N_2 . As nitrate concentrations are lowered, microbial reduction series continue through other electron acceptors, like manganese and iron oxides and sulphates. Classical redox reaction sequences are often found along groundwater flow paths in large aquifers [8], with denitrified waters observed at greater depth [9]. Denitrification can also occur in the gas-filled unsaturated zone if microbial oxygen consumption far exceeds the rate of diffusive oxygen replenishment from the air to create anoxic soil conditions [10]. Declining NO_3^- concentrations at depth are generally observed in unsaturated [11] or saturated zones [12–14]. Discrepancies between the expected and simulated NO_3^- concentrations in groundwater recharging from the soil zone are often observed [10], and often have a seasonal pattern [15]. On the other hand, increasing trends of nitrate concentrations in groundwater are attributed to stored nitrate in the subsurface and its potential long travel time (decades) in thick unsaturated zones before reaching the water table [15,16].

Dual isotope analysis of nitrate ($\delta^{15}\text{N}\text{-NO}_3^-$ and $\delta^{18}\text{O}\text{-NO}_3^-$) provides a powerful tool to discriminate sources of nitrate in aquatic ecosystems, but their application becomes often complicated due to overlapping and multiple N sources as well as subsequent biogeochemical processes that alter the source signatures [17–24]. The $\delta^{15}\text{N}\text{-NO}_3^-$ values can be linked to distinctive N sources [25]: (1) ammonium synthetic fertilizers (–10 to +5 ‰), (2) soil nitrate (+2 to +9 ‰) and (3) animal and septic waste (0 to +25 ‰). The $\delta^{18}\text{O}\text{-NO}_3^-$ values are typically < +15 ‰, or between +17 and +25 ‰ when nitrate synthetic fertilizers are present and >+25 ‰ when nitrogen pollution originates from atmospheric deposition [20,26,27]. In rivers, biogeochemical processes occur at the oxic/anoxic river sediment–water interface, but also at the interface of water with the suspended particles at the flowing water [28]. River water is typically aerobic due to rapid gas exchange with the atmosphere and thereby favouring nitrification, whereas the subsurface sediments are limited by oxygen flux and become anaerobic, which favours nitrate removal (e.g. denitrification, anammox and dissimilatory nitrate reduction to ammonium (DNRA)). Nitrate attenuation in rivers is also possible by assimilation, namely the acquisition of N in aquatic organisms resulting in isotope fractionation on the NO_3^- substrate yielding a ca. 1:1 change in the $\delta^{18}\text{O}\text{-NO}_3^-:\delta^{15}\text{N}\text{-NO}_3^-$ [25]. Nitrate in the aquifers is preferentially processed through a denitrification sequence ($\text{NO}_3^- \rightarrow \text{N}_2$), resulting in heavy isotope enrichment of ^{18}O and ^{15}N in the residual substrate, a process that generally follows a $\delta^{18}\text{O}\text{-NO}_3^-:\delta^{15}\text{N}\text{-NO}_3^-$ ratio of 1:2 [20]. The reaction chain in the aerobic unsaturated zone includes ammonification and finally the conversion of ammonium to nitrate (nitrification), resulting in relatively lower $\delta^{15}\text{N}\text{-NO}_3^-$ values with increasing NO_3^- -N concentration [25].

Denitrification processes in aquifers are widespread, but not universal. Clague et al. [10] identified nitrate reduction processes in phreatic aquifers close to the water table, indicating that reduction processes are likely to have started in the unsaturated zone. Wu et al. [29] showed that low permeability sediments have high nitrate reduction potential enhancing nitrate denitrification in aquifers. Higher denitrification rates in aquifers are linked to increasing electron donors for O_2 reduction, such as organic carbon and sulfide deposits (e.g. [30,31]). Groundwater fed rivers often show high nitrate concentrations during high flow or under cold season conditions when much of the groundwater is transmitted rapidly across the riparian zone, and low nitrate concentrations during low flow conditions when stream discharge is dominated by recharge from the deeper denitrified parts of the aquifer [32]. Weitzman et al. [33] showed that variable NO_3^- concentration and isotope ($\delta^{15}N-NO_3^-$ and δ^2H-H_2O) values in groundwater are indicators of mixing, whereas variable NO_3^- concentration and $\delta^{15}N-NO_3^-$ values and constant δ^2H-H_2O values are indicators of denitrification.

In this study, we assessed the source and biogeochemical transformations of nitrate in a spring-fed stream and catchment crossing an agricultural and partly urbanized landscape near Vienna, Austria (Figure 1). We investigated in-stream nitrate transformations and sources on a seasonal basis, as the stream lost and gained flow from the underlying phreatic groundwater system. We elucidated sources of nitrate from the slightly nitrate contaminated source spring and along the river flow path to the confluence with the Danube River by using $\delta^{15}N$ and $\delta^{18}O$ of NO_3^- and water isotopes ($\delta^{18}O$ and δ^2H of H_2O) covering a full hydrological year (2019–2020).

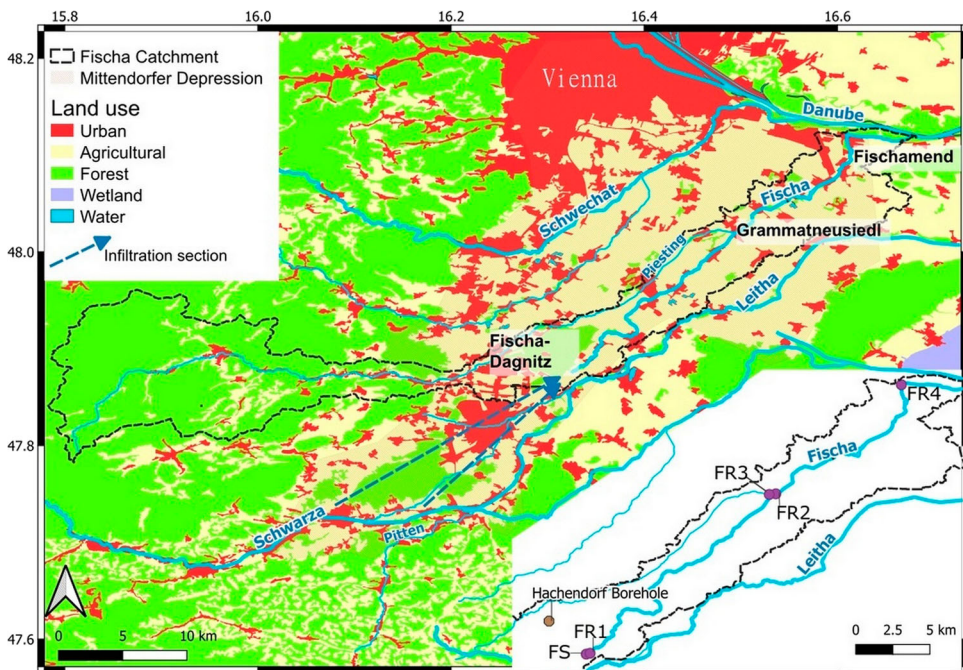


Figure 1. Map of the study area and the sampling sites (Land-uses are from [39]). FS refers to the Fischa-Dagnitz spring water site, whereas FR1–FR4 to river water sites.

2. Materials and methods

2.1. Study area

The Fischa-Dagnitz spring and catchment are located ~35 km south of Vienna, Austria, and belong to the southernmost part of the Vienna basin, including the Mitterndorfer depression aquifer (Figure 1). The Mitterndorfer depression aquifer is south of the Danube River and is composed by sequences of coarse and fine late Quaternary alluvial sediments [34,35]. The surficial sediments have an average thickness of 175 m and host one of the largest groundwater reservoirs in Europe. The aquifer is mostly recharged (75 %) from the Alpine region through the fractured karst aquifer of Northern Calcareous Alps west and below the Vienna basin, and ca. 25 % from local precipitation (600 mm/a) [36,37]. The Fischa-Dagnitz system has three distinctive source springs located within 200 m from each other, forming from their discharge a first-order stream. Over the first kilometre, the Fischa River is fed by upwelling groundwater before it confluent with the Neue Fischa Pottendorf tributary. After ~10 km the river confluent with the Piesting River and eventually merges with the Danube River at Fischamend.

The spring water system is mainly recharged from the Schwarza and Pitten River by infiltrating into gravel deposits ca. 20 km away from the Fischa springs, and less from precipitation and irrigation return flow [38]. However, an additional contribution of much older groundwater from the Alpine karst was previously identified [37]. Groundwater dating with tritium shows that around 20 % of the water is very young (≤ 3 –4 years old) and 80 % is mixed with older water (> 20 years old) [36]. Stream discharge rate rises rapidly from ca. 54 l/s at Fischa-Dagnitz springs (FS) to ca. 679 l/s at the Grossmittler Road bridge located ca. 1900 m downstream. Land use in the catchment is mainly agricultural (~55 %), forest (~27 %) and urban (~18 %) [39]. Nitrate (NO_3^-) concentrations in the Fischa springs area are generally low (on average ~3.7 mg/L as NO_3^- -N, at about 1800 m downstream of spring waters, close to the town of Haschendorf), below the threshold set by WHO (11.3 mg/l as NO_3^- -N, [6]) and with a decreasing trend over the years [40].

2.2. Sampling and analysis

Five sites (Figure 1) were selected for physical–chemical parameters and stable isotopes on a monthly basis from September 2019 to November 2020. All five sites were collected within one day in every campaign. In total, 61 water samples were collected over one year. The FS sampling site was the Fischa-Dagnitz spring where groundwater discharges to form a stream, whereas the rest of the sites were river water sampling sites (FR1–FR4) up to the confluence with the Danube River at Fischamend. *In situ* parameters recorded were temperature, pH and electrical conductivity measured by means of a HACH multi-meter instrument. River water discharge (in m^3/s) data at Fischamend was obtained from MA31 Wiener Wasser.

Water samples for chemical and stable isotope analyses were field filtered through 0.45 μm filters and stored cold in 50 mL HDPE bottles and transported to the laboratory. Nitrate isotope samples were stored frozen to avoid biodegradation until isotope analysis. All samples were analysed for their N chemical composition within a few days of collection. Nitrate, nitrite and ammonium content analysis followed the standard methods 4500-NH₃ G APHA [41] using a discrete analyzer (AQ1, Seal Analytical, Germany) and

an ion chromatography system. Nitrate, nitrite and ammonium concentrations were reported in mg/l as NO_3^- -N, NO_2^- -N and NH_4^+ -N. For nitrate ^{15}N and ^{18}O isotopes, samples were analysed in the IAEA Isotope Hydrology Laboratory by using the Ti(III) reduction method [42], which directly converts aqueous nitrate to N_2O headspace gas in septum capped vials. The N_2O in the headspace was measured for $^{15}\text{N}/^{14}\text{N}$ and $^{18}\text{O}/^{16}\text{O}$ ratios using a CF-IRMS (Isoprime-100 Trace Gas Analyser, Elementar, UK). None of the samples had NO_2^- concentrations above the instrumental detection limit (0.01 mg/l-N), and hence no correction for nitrite in the Ti(III) reduction method was required. Water isotope analysis (^{18}O - H_2O , ^2H - H_2O) was conducted on the same water samples that were used for nitrate isotope analysis by laser spectroscopy at the IAEA using a Los Gatos Research liquid-water isotope analyzer (TLWIA-912).

The stable isotope ratios were expressed in delta (δ) and per mil (‰) notation relative to an international standard [43]:

$$\delta(\text{‰}) = \left(\frac{R_{\text{sample}}}{R_{\text{reference}}} - 1 \right) \times 1000, \quad (1)$$

where R_{sample} and $R_{\text{reference}}$ are the ratios of $^{15}\text{N}/^{14}\text{N}$, $^{18}\text{O}/^{16}\text{O}$, $^2\text{H}/^1\text{H}$ in a sample and the international reference, respectively. Atmospheric N_2 was the isotopic reference for nitrogen and the Vienna Standard Mean Ocean Water (VSMOW) for oxygen (of NO_3^- and H_2O) and hydrogen. Analytical uncertainties were ± 0.5 ‰ for $\delta^{15}\text{N}$ - NO_3^- and $\delta^{18}\text{O}$ - NO_3^- , and ± 0.1 ‰ and ± 0.4 ‰ for $\delta^{18}\text{O}$ and $\delta^2\text{H}$, respectively.

2.3. Hydrological data

Rainfall data for the same sampling period (September 2019–November 2020) was obtained from the Wiener Neustadt meteorological station (Lat: 47.83°, Long: 16.21°, Elevation 285 m.a.s.l.) at a distance of ~ 5 km SW of the FS site. Given that daily precipitation data were available, the precipitation amount for each month was calculated for a period of 2 weeks before the sampling date. Groundwater levels for the same period of sampling were obtained from the Haschendorf Blt 379 (Fischa) borehole (Lat: 47.906°, Long: 16.292°, Elevation 253.2 m.a.s.l., [44]) located at a distance of ~ 800 m north of Fischa-Dagnitz springs. Nitrogen loadings (kg/d) at Fischamend were calculated based on the following equation:

$$\text{Nitrogen loadings (kg/d)} = \text{N-compound (mg/L)} \times \text{Discharge (m}^3/\text{s)} \times 1.44 \quad (2)$$

Given that most measured NO_2^- -N and NH_4^+ -N values were below instrumental detection limits, only NO_3^- -N concentration was used for the calculation of the nitrogen loadings.

2.4. Isotope data processing and modelling

2.4.1. Biogeochemical processes

The ^{15}N isotopic enrichment factor (ϵ) for denitrification is defined as [43]:

$$\epsilon = (\alpha - 1)1000, \quad (3)$$

where $\alpha = R_{\text{N}_2}/R_{\text{NO}_3}$, R_{N_2} is the isotope ratio of the reaction product (N_2), and R_{NO_3} is the isotope ratio of the reaction substrate (residual NO_3^-). The Rayleigh equation describes the

evolution of the isotopic composition of the residual NO_3^- where the products are removed from chemical or isotope equilibrium with the reactant. A simplified version of the Rayleigh equation is [43]:

$$\delta \sim \delta_0 + \varepsilon \ln(f), \quad (4)$$

where δ is the isotopic composition of the substrate, δ_0 is the initial isotopic composition of the substrate, ε is the enrichment factor and f is the remaining fraction of the substrate.

Denitrification percentages (f) were estimated using an average isotope fractionation of $\varepsilon_{\text{NO}_3-\text{N}_2}^{15} = 15 \text{‰}$ [45] and a $\varepsilon_{\text{NO}_3-\text{N}_2}^{18} / \varepsilon_{\text{NO}_3-\text{N}_2}^{15}$ ratio of 0.7 [20]. We considered a $\delta^{15}\text{N}-\text{NO}_3^-$ value of +5 ‰, as the original nitrate source that could be related to soil organic matter in temperate climates [46] or to NH_4^+ synthetic fertilizers with the highest $\delta^{15}\text{N}-\text{NO}_3^-$ values reported [20,47] and randomly three $\delta^{18}\text{O}-\text{NO}_3^-$ values within the range of measured values in FS site (between -1.0 and $+4.0 \text{‰}$) [20,48].

The influence of ^{18}O in water and molecular O_2 on the ^{18}O of NO_3^- produced during nitrification was described using an isotope mass balance [20]:

$$\delta^{18}\text{O}-\text{NO}_3^- = 2/3 \delta^{18}\text{O}-\text{H}_2\text{O} + 1/3 \delta^{18}\text{O}-\text{O}_2, \quad (5)$$

where $\delta^{18}\text{O}$ of O_2 was assumed to be in equilibrium with air ($+24.2 \text{‰}$) [49].

2.4.2. Modelling

To reduce the influence of variability of liquid water isotopes, the $\delta^{18}\text{O}-\text{NO}_3^-$ values were normalized to *in situ* $\delta^{18}\text{O}-\text{H}_2\text{O}$ for the application of an isotope mixing model only for FS site, as follows [50]:

$$\delta^{18}\text{O}-\text{NO}_3^- \text{ normalised} = \frac{\delta^{18}\text{O}-\text{NO}_3^- + 1}{\delta^{18}\text{O}-\text{H}_2\text{O} + 1} - 1 \quad (6)$$

A two end-member mixing model was applied using a mass balance equation:

$$\delta^{15}\text{N}_{\text{sw}} \cdot \delta^{18}\text{O}_{\text{sw(normalised)}} = f_1(\delta^{15}\text{N}_{\text{soil}} \cdot \delta^{18}\text{O}_{(\text{soil})\text{normalised}}) + f_2(\delta^{15}\text{N}_{\text{bc}} \cdot \delta^{18}\text{O}_{(\text{bc})\text{normalised}}) \quad (7)$$

The mole fraction f_1 refers to soil contribution. Considering that $f_1 + f_2 = 1$, the mole fraction f_2 of baseflow (denitrified) water was calculated by:

$$f_2 = \frac{\delta^{15}\text{N}_{\text{soil}} \times \delta^{18}\text{O}_{(\text{soil})\text{norm}} - \delta^{15}\text{N}_{\text{sw}} \times \delta^{18}\text{O}_{(\text{sw})\text{norm}}}{\delta^{15}\text{N}_{\text{soil}} \times \delta^{18}\text{O}_{(\text{soil})\text{norm}} - \delta^{15}\text{N}_{\text{bc}} \times \delta^{18}\text{O}_{(\text{bc})\text{norm}}} \quad (8)$$

The $\delta^{15}\text{N}_{\text{bc}}$ and $\delta^{18}\text{O}_{(\text{bc})\text{norm}}$ refer to the nitrate isotope values in August baseflow conditions (bc), the $\delta^{15}\text{N}_{\text{soil}}$ and $\delta^{18}\text{O}_{(\text{soil})\text{norm}}$ refer to the nitrate isotope values in May (when $\delta^{15}\text{N}-\text{NO}_3^-$ was close to a soil value of +5 ‰) and the $\delta^{15}\text{N}_{\text{sw}}$ and $\delta^{18}\text{O}_{(\text{sw})\text{norm}}$ refer to the nitrate isotope values of the spring water (sw) in all other months. We did not consider the $\delta^{18}\text{O}$ and $\delta^{15}\text{N}$ of NO_3^- in rain, given that precipitation nitrogen is cycled quickly in contact with soil surface and subsurface [25]. The uncertainty in the calculation of f_2 was determined by trying the $\delta^{15}\text{N}_{\text{soil}}$ values of +2 ‰ and +9 ‰, which correspond to the minimum and maximum $\delta^{15}\text{N}-\text{NO}_3^-$ soil values [25], and the analytical uncertainty of $\pm 0.5 \text{‰}$ in the $\delta^{15}\text{N}_{\text{bc}}$ value.

A least-square linear regression model was applied to investigate relationships between variables. All linear regression models were evaluated by examining the goodness of fit and the significance of the slopes. A conventional probability value (p -value) of 0.05 was used to indicate significance. All statistical tests were done using R v.3.3.270.

3. Results

3.1. Physical–chemical, isotopic ($\delta^{18}\text{O}$ and $\delta^2\text{H}$ of H_2O) and hydrological parameters

3.1.1. Physical–chemical results

The EC values ranged between 328 and 550 $\mu\text{S}/\text{cm}$, with an average value of ~ 450 $\mu\text{S}/\text{cm}$. Water temperature and pH averaged ~ 15 $^\circ\text{C}$ and ~ 8 pH units, respectively, with the highest pH and water temperature values recorded in autumn and summer months, respectively (Table S1, Figure S1). Nitrate concentration values in spring and river waters ranged between 0.6 and 3.7 mg/L of NO_3^- -N with a minimum concentration in August (Table S1, Figure S2). The average nitrate concentration at the FS site during the observational period was 3.3 mg/l of NO_3^- -N, with a difference of only 1 mg/l between maximum and minimum value over the year (Figure 2). A minimum value of 2.7 mg/l NO_3^- -N was recorded under baseflow conditions in August. Similar nitrate concentration values were recorded at the FR1 site, with an average of 3.2 mg/l of NO_3^- -N and a difference of 1.6 mg/l of NO_3^- -N between the minimum and maximum value (Table S1). The average nitrate concentration at all other sites (FR2–FR4) ranged between 1.3 mg/l of NO_3^- -N at the FR3 site and 2.4 mg/l of NO_3^- -N at the FR4 site (Table S1, Figure 3). Ammonium (NH_4^+) exhibited values below detection limit for most sites.

3.1.2. Water isotopes ($\delta^{18}\text{O}$ and $\delta^2\text{H}$ of H_2O)

The $\delta^{18}\text{O}$ - H_2O values at FS site were stable (ranging from -10.5 to -10.2 ‰) throughout the year, with slightly higher values in summer and lowest in winter (-10.9 ‰ in January). A similar $\delta^{18}\text{O}$ - H_2O minimum in January was recorded at the FR1 and FR2 sampling sites (Figures 2 and 3). Similarly, the $\delta^{18}\text{O}$ - H_2O values were stable at the FR3 (between -10.5 and -10.3 ‰) and FR4 (between -10.4 and -10.3 ‰) sites, with the lowest peaks recorded in winter and the highest in summer (Figure 3). The water isotopic compositions were plotted against the Global and the Vienna Meteoric Water Lines (Figure 4) and compared to the long-term weighted water isotope values of precipitation in Vienna [51–53]. We obtained precipitation isotope data for Vienna from the IAEA-GNIP database (www.iaea.org/water).

3.1.3. Hydrological results

The groundwater table at the Haschendorf borehole located near the FS sampling site showed a decreasing trend into summer and an increasing in winter. However, although precipitation amount values > 40 mm were recorded in summer, groundwater levels did not respond and stayed low in August despite two periods of intense precipitation throughout June and July. The groundwater level started to rise in September and continued to rise till November, despite the low precipitation during that month (Figure 2).

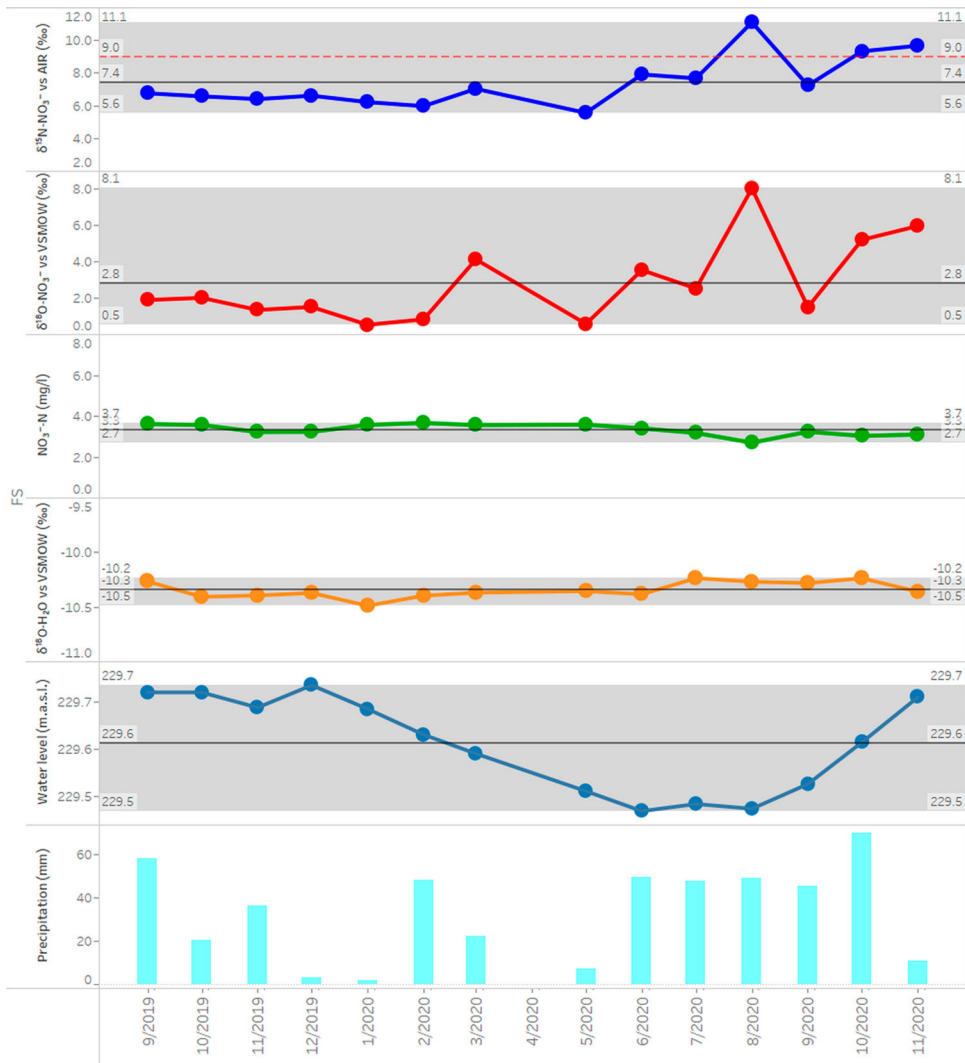


Figure 2. Temporal variation of isotope and nitrate variables at Fische-Dagnitz spring water site (FS), the water level at Haschendorf borehole and the precipitation amount (2 weeks prior to sampling date) at Wiener Neustadt meteorological station. Grey shaded area indicates the range of values and the red striped line the $\delta^{15}\text{N-NO}_3^-$ threshold of +9‰, above which organic pollution is the dominant nitrate source [20].

Discharge at the FR4 site showed relatively low values (4.2–4.5 m³/s) during July–August (Figure S3), with the lowest total N loadings (11.0 kg/d) and highest EC values (550 $\mu\text{S}/\text{cm}$) recorded in August. The lowest discharge value (3.8 m³/s) was in May 2020, with relatively low total N loading (15.8 kg/d) and high EC (542 $\mu\text{S}/\text{cm}$) values.

3.2. Nitrate isotopes ($\delta^{15}\text{N}$, $\delta^{18}\text{O}$ of NO_3^-)

3.2.1. Temporal variation

Considering the overall temporal evolution of the isotope variables of all sites together, the nitrate isotope values showed greater variation (range: 9.1‰) compared to NO_3^- -N



Figure 3. Temporal variation of isotope and nitrate concentration variables at the sampling sites.

concentrations (range: 3.1 mg/L) (Figure S2). Nitrate isotopes showed no significant seasonal variation (not shown here) but averaged highest in August and lowest values in May and February.

The isotopic composition of nitrate at the FS sampling site, however, exhibited a significant isotope variability on a seasonal basis, with the highest $\delta^{15}\text{N}$ and $\delta^{18}\text{O}$ values in summer and particularly in August (+11.1 and +8.1 ‰, respectively) and the lowest values in January and May (+5.5 to +6.2 ‰ and \sim +0.5 ‰, respectively) (Figure 2).

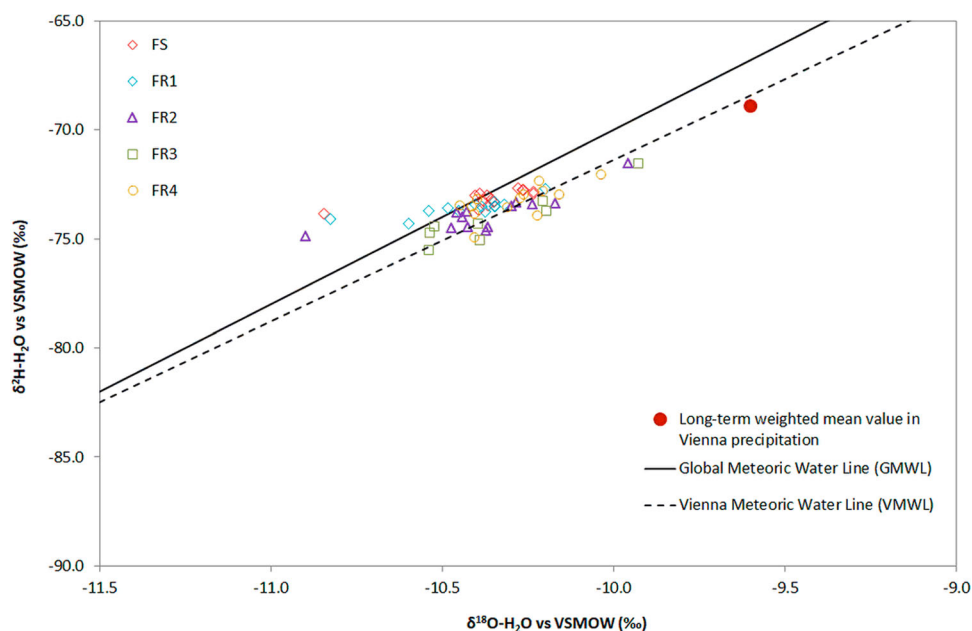


Figure 4. Plot of $\delta^{18}\text{O-H}_2\text{O}$ vs $\delta^2\text{H-H}_2\text{O}$. GMWL is after [51]. VMWL is after [52]. The data for the calculation of the long-term weighted values was taken from IAEA/WMO GNIP [53].

Contrary to the negligible variability of nitrate concentrations over this monitoring period, the $\delta^{15}\text{N-NO}_3^-$ and $\delta^{18}\text{O-NO}_3^-$ values exhibited a high variability of +5.5 and +7.6 ‰, respectively.

The FR1 site is a gaining stream located ~350 m downstream of FS site. The temporal variation of NO_3^- concentration and nitrate isotope values was similar to FS water site, with high, but lower than the spring water, peaks of $\delta^{15}\text{N}$ and $\delta^{18}\text{O}$ of NO_3^- in August (Figure 3). A high $\delta^{18}\text{O-NO}_3^-$ peak was observed in March.

A $\delta^{15}\text{N-NO}_3^-$ peak of August at the FS and FR1 sites was detected but dampened at the FR2 and FR4 sites during low discharge and N loading conditions. At the FR3 site, $\delta^{15}\text{N-NO}_3^-$ values peaked in August and September (Figure 3). These patterns became clearer when examining the relationships during baseflow period (August–September, Figure S4). The FR4 site peaked highest $\delta^{15}\text{N-NO}_3^-$ value (+13.1 ‰) in December and higher $\delta^{15}\text{N-NO}_3^-$ value (+9.2 ‰) compared to the upstream sites and the Danube at Hainburg site [54] in July (Figure S5).

3.2.2. Spatial variation

Regardless of the season, the chemical and isotopic composition from the Fischa-Dagnitz area (FS1 and FR1) showed higher average NO_3^- -N concentration and lower average $\delta^{15}\text{N-NO}_3^-$ and $\delta^{18}\text{O-NO}_3^-$ values compared to downstream sites (FR3–FR5) (Figure 5). The FR3 site belongs to a tributary of Fischa stream, mainly recharged in the Piesting area, which exhibited the lowest average NO_3^- -N concentration and the highest average $\delta^{15}\text{N-NO}_3^-$ and $\delta^{18}\text{O-NO}_3^-$ values. The FR4 site showed similar average value of NO_3^- -N concentration and $\delta^{15}\text{N}$, $\delta^{18}\text{O-NO}_3^-$ with FR2 after the confluence with FR3.

3.2.3. Origin of nitrate

All samples from sites FR1–FR4 plotted within the overlapping source ranges of soil and anthropogenic wastes/manure fields, apart from some samples from the tributary (FR3) and the Fischamend (FR4) that plotted within the anthropogenic wastes or manure field (Figure 6). All samples of the FS site plotted within the overlapping ranges of soil and anthropogenic wastes/manure fields, apart from the August, October and November samples, which showed a clear anthropogenic organic origin ($\delta^{15}\text{N-NO}_3^- > +9$ ‰). The samples of the FR1 site were plotted within the overlapping ranges of soil and anthropogenic wastes/manure fields.

3.2.4. Correlations and biogeochemical and mixing processes

A positive correlation ($R^2 = 0.91$, $p < 0.05$) at the FS site had a slope of ~ 1.4 , whereas the relationship between $\delta^{15}\text{N}$ and $\text{NO}_3^- \text{-N}$ values was significantly negative with $R^2 = 0.73$ (Figures 6 and 7). The FR1 site showed a positive correlation ($R^2 = 0.73$) between $\delta^{15}\text{N-NO}_3^-$ and $\delta^{18}\text{O-NO}_3^-$ values with a slope of ~ 1.1 (Figure 6), and a significant but weaker ($p < 0.05$, $R^2 = 0.35$) negative correlation of $\delta^{15}\text{N-NO}_3^-$ with $\text{NO}_3^- \text{-N}$ concentration compared to the spring water site (Figure 7). The

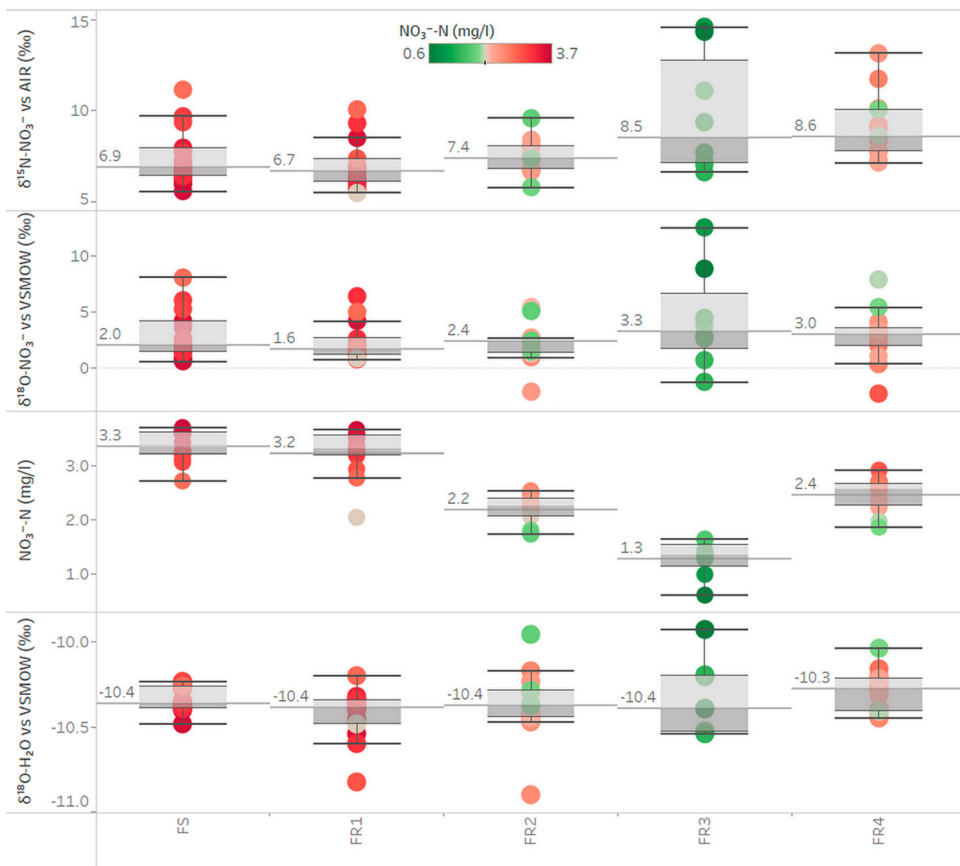


Figure 5. Spatial evolution of chemical and isotopic variables from the Fischa-Dagnitz spring water site (FS) till Fischamend area (FR4).

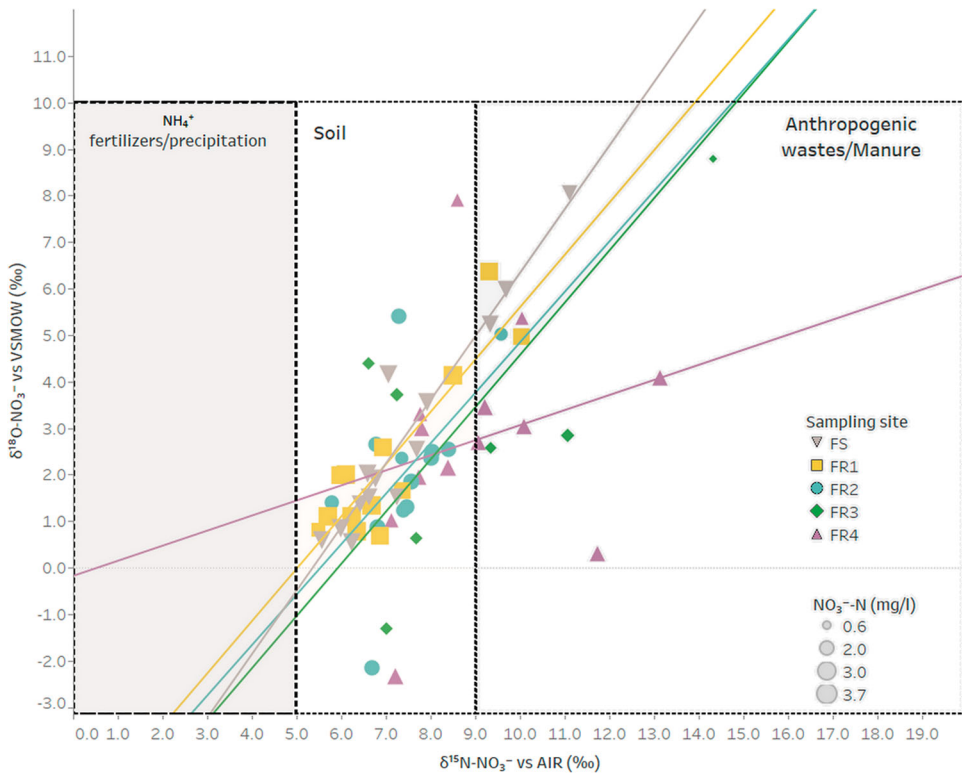


Figure 6. Bivariate $\delta^{15}\text{N-NO}_3^-$ vs $\delta^{18}\text{O-NO}_3^-$ plot of the sampling sites. Nitrate source ranges are after [25].

FR3 site showed a significant positive correlation ($p < 0.05$, $R^2 = 0.67$) between $\delta^{15}\text{N-NO}_3^-$ and $\delta^{18}\text{O-NO}_3^-$ with a slope of ~ 1.1 , which became more significant when the growing period between May and September was examined. The FR2 and FR4 sites showed significant positive correlation ($p < 0.05$) between $\delta^{15}\text{N-NO}_3^-$ and $\delta^{18}\text{O-NO}_3^-$ values, particularly during the growing season with slopes > 1.5 . Only FR1 and FR3 river sites showed a significant ($p < 0.05$) and negative correlation between $\delta^{15}\text{N-NO}_3^-$ and NO_3^- -N values (Figure 7).

Spring and stream water samples showed variable deviations from a nitrification line (Figure 8). In particular, the samples of the FS site were close to the nitrification line during January and February, whereas for other sites the deviation from the line was lowest during the autumn and winter months. The highest positive deviations from the nitrification line were observed in August and September. Stream waters of May (for FR2 and FR4 sites) and October (for FR3 site) showed the highest negative deviations from the nitrification line.

A denitrification model for the FS site showed that samples have undergone differential denitrification as expressed by the NO_3^- residual value (f_2) with the highest NO_3^- residual value ($f_2 = 0.68$) observed during August (Figure 9). The results of the mixing model showed that baseflow contribution was variable throughout the year, with the highest contribution ($\sim 53\%$) during summer and the lowest during winter ($\sim 7\%$) (Figure 10).

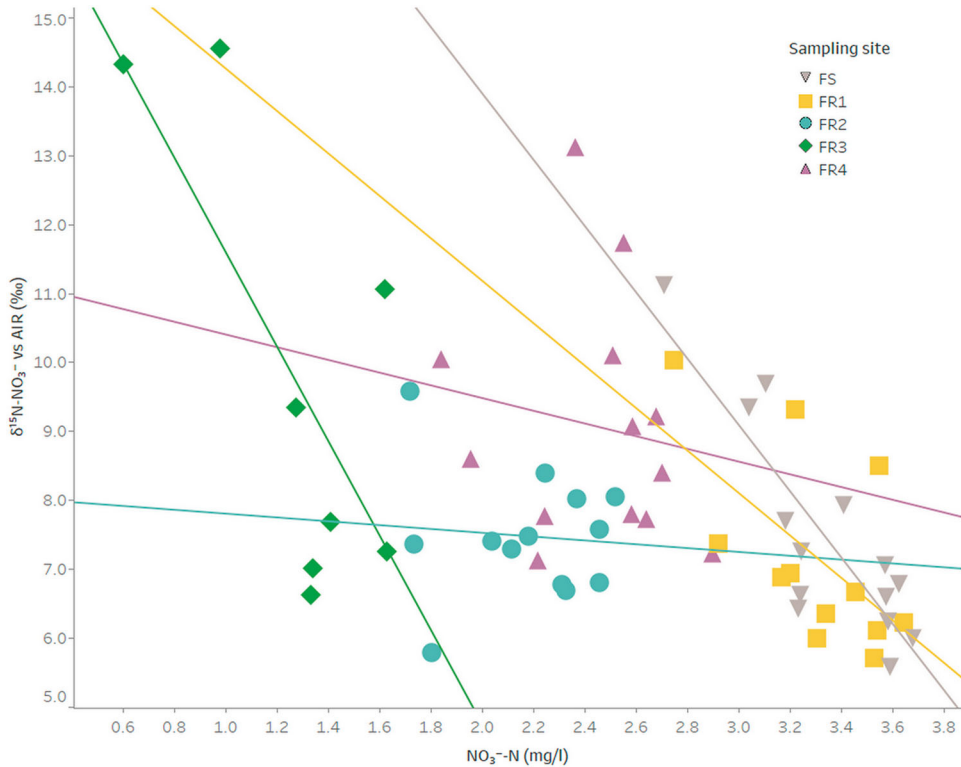


Figure 7. Bivariate $\delta^{15}\text{N-NO}_3^-$ vs NO_3^- -N plot of the sampling sites.

4. Discussion

4.1. Overall patterns

The temporal evolution of the NO_3^- -N concentration at all monitoring sites showed very little variation, which could be interpreted as a steady-state nitrate source contribution throughout the year, yet the considerable range in nitrate isotopes revealed variable biogeochemical processes. These processes probably mask the original nitrate sources, which is a mixture of soil, anthropogenic wastes/manure and fertilizers. The overall high $\delta^{18}\text{O-NO}_3^-$ peaks in March, August and September were attributed to a stronger precipitation signal and/or respiration processes in the unsaturated zone and the ecosystems [55]. On the other hand, the relatively low $\delta^{18}\text{O-NO}_3^-$ peaks of January, February, May and October were due to nitrification and/or increased photosynthetic processes in the streams, as evidenced by the small deviation from the nitrification line [55]. The $\delta^{18}\text{O-NO}_3^-$ peaks of January coincided with low $\delta^{18}\text{O-H}_2\text{O}$, which could indicate a mixing of older Alpine source waters (of high d -excess) and basin precipitation. Full equilibration or O-isotope exchange of NO_2^- with H_2O before being oxidized to NO_3^- in soils and rapid redox cycling between NO_3^- and NO_2^- can also potentially increase $\delta^{18}\text{O-NO}_3^-$ values [56–58].

The isotope contents of the Fischa-Dagnitz system (~ -10.5 ‰ for $\delta^{18}\text{O-H}_2\text{O}$ and ~ -74 ‰ for $\delta^2\text{H-H}_2\text{O}$) were on average depleted by ~ 0.8 ‰ compared to the long term

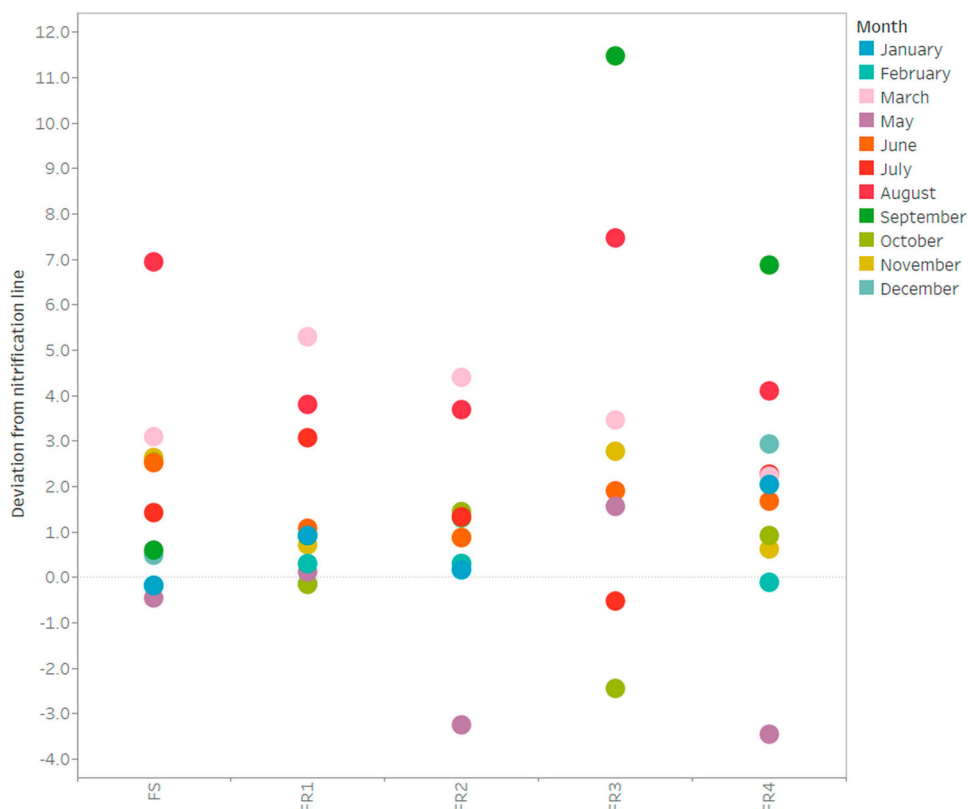


Figure 8. Deviation of observed $\delta^{18}\text{O-NO}_3^-$ values from the theoretical $\delta^{18}\text{O-NO}_3^-$ values for nitrification considering 2:1 for water:oxygen contribution from FS till FR4 site.

$\delta^{18}\text{O-H}_2\text{O}$ value for the Vienna GNIP station (-9.6‰), reflecting the importance of recharge sources located at higher elevation. This isotopically depleted signal is slightly modified (Figure 4) towards more enriched values along the stream until the confluence with the Danube River, reflecting the importance of groundwater discharge in the system.

4.2. Fische-Dagnitz springs area – FS and FR1

Despite the low variability of nitrate concentrations throughout the year, the $\delta^{15}\text{N-NO}_3^-$ and $\delta^{18}\text{O-NO}_3^-$ values at FS site exhibited a high spatiotemporal variability well beyond measurement uncertainties. The nitrate isotope data showed that nitrate contamination was attributable to soil and anthropogenic wastes/manure fields. However, considering the main land-uses in the area and given that manure is not applied, it seems unlikely that the high nitrate isotope values especially in August can be attributed to manure or to anthropogenic waste sources. On the contrary, mineral synthetic fertilizers have been applied in the basin for many years. However, their isotopic signal was impossible to detect due to nitrogen recycling after its initial fixation from N_2 (either biological or Haber–Bosch), as biogeochemical processes bring reactive N in the plant–soil–water continuum of the unsaturated zone with a ^{15}N value of $\sim 0\text{‰}$ [59]. Thus, mineral fertilizers and

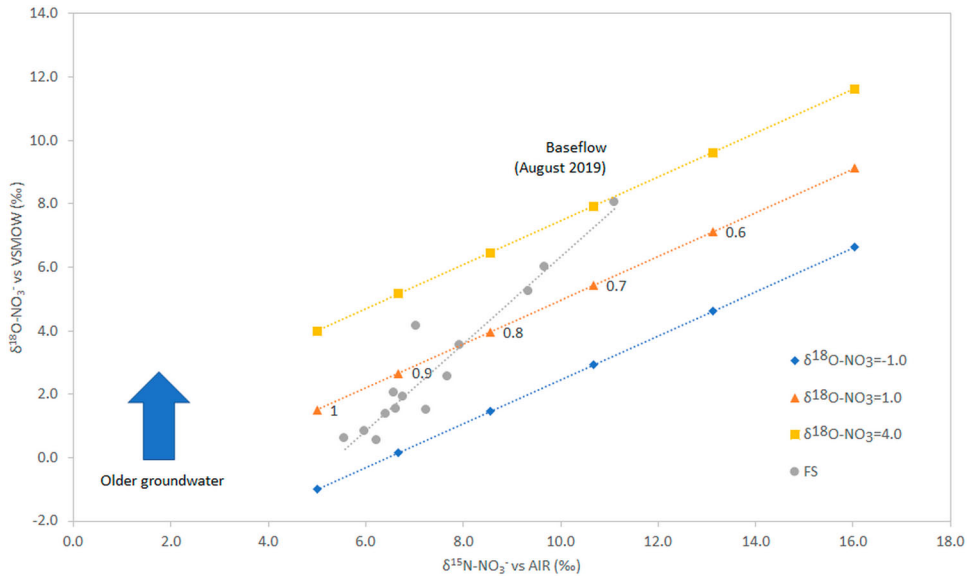


Figure 9. Denitrification model for the FS site for different starting points. The numbers along the denitrification line refer to the residual NO_3^- (f).

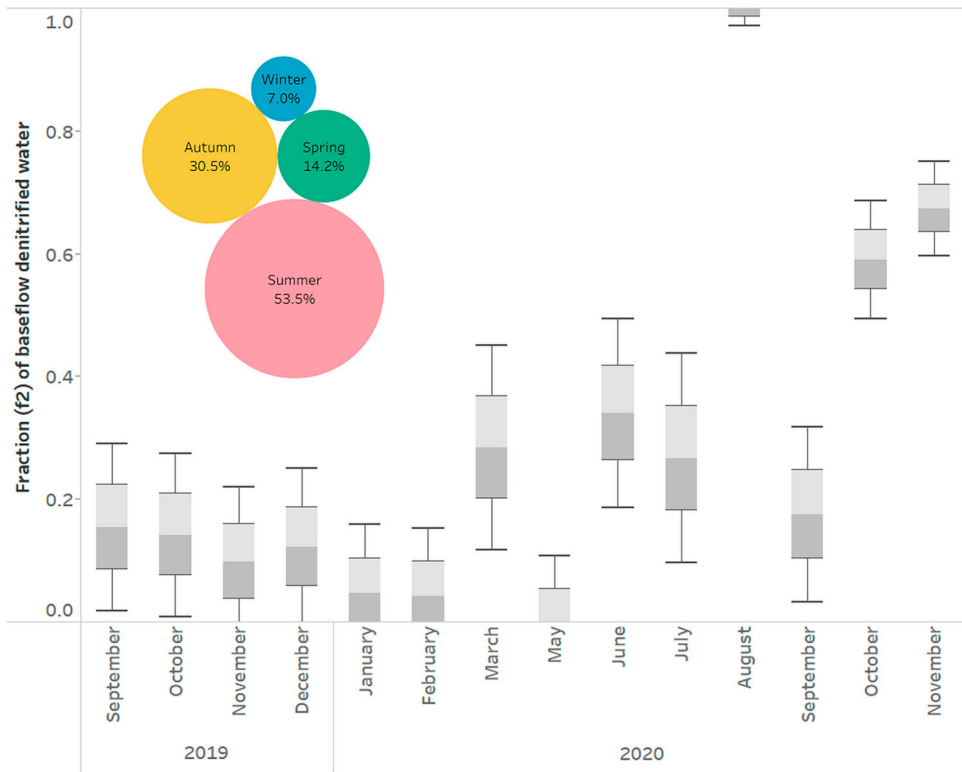


Figure 10. Baseflow contribution at the FS site. The error bars represent the uncertainty.

soil N sources are likely responsible for the nitrate isotope values; however, given that the samples at the FS site gave a positive time trend line, it is possible that biogeochemical processes have altered the initial isotopic signal. The nitrate concentrations at the FS site were almost constant and slightly above the nitrate expected from natural soil [60], which could be related to the long-term application of fertilizers migrating through the unsaturated zone [33].

Given that deeper groundwaters may undergo denitrification due to the reduced oxygen levels [7], the significant negative correlation between $\delta^{15}\text{N-NO}_3^-$ and NO_3^- -N concentration values at the FS site affirmed the influence of denitrification. However, the correlation between $\delta^{15}\text{N-NO}_3^-$ and $\delta^{18}\text{O-NO}_3^-$ values showed a much higher $\delta^{15}\text{N-NO}_3^-:\delta^{18}\text{O-NO}_3^-$ ratio (>1.0) than the typical ratio (0.5–0.7) [20] expected for denitrification. A $\delta^{15}\text{N-NO}_3^-:\delta^{18}\text{O-NO}_3^-$ ratio of 1.0 for denitrification has been detected experimentally but not in real freshwater systems [57]. Thus, this trend line is likely a result of mixing between aquifer water of different depths and denitrification ranging from 0.9–0.68 of residual NO_3^- . This implies that the older the groundwater, the more denitrified this groundwater discharged through the spring is. This pattern was supported by the highest $\delta^{15}\text{N}$ and $\delta^{18}\text{O}$ values of NO_3^- and the lowest NO_3^- concentration of baseflow conditions in August 2020. The lowest groundwater levels recorded at the Haschendorf borehole supported the reduced recharge of the springs from precipitation for this period of the year. However, given that the FS site is partly fed by the Schwarza River, N fractionation due to assimilation prior to river water infiltration should not be excluded and further investigation is warranted.

A mixing model showed that old groundwater contributes to $> 50\%$ to spring discharge during summer, with an uncertainty of $\pm\sim 13\%$. The Mean Transit Time models of Stolp et al. [38] confirm discharge of decades-old groundwater at FS, with Kralik and Stewart [61] estimating the fraction of old groundwater of $\sim 75\%$, based on tritium and water isotope data. An increase in the $\delta^{15}\text{N-NO}_3^-:\delta^{18}\text{O-NO}_3^-$ ratio due to other nitrate depletion mechanisms such as DNRA and assimilation of nitrate into microbial biomass are unlikely to be important in subsurface settings relative to denitrification [7]. Moreover, when considering precipitation amount in comparison with the groundwater level, the latter did not respond immediately, requiring two months for the system to respond. This means that nitrate contamination in the recharge area is not immediately reflected in the spring discharge.

The FR1 site located 350 m downstream of the FS site showed similar average and temporal variation of chemical and isotope species, which confirmed recharge by the spring waters. The relationship of $\delta^{15}\text{N-NO}_3^-$ with $\delta^{18}\text{O-NO}_3^-$ and NO_3^- -N concentration again revealed the denitrification pattern, but with lower peaks compared to the FS site, which indicated that the denitrification signal of groundwater from the springs, although detectable, was dampened downstream due to mixing with less or non-denitrified surface waters.

4.3. Downstream of the Fischa-Dagnitz springs area – FR2–FR4

Downstream of the Fischa-Dagnitz springs area the $\delta^{15}\text{N-NO}_3^-$ and $\delta^{18}\text{O-NO}_3^-$ values increased, whereas NO_3^- concentration decreased. At the downstream sites, the nitrate source origin is mostly soil and anthropogenic wastes/manure. However, the correlation between $\delta^{15}\text{N-NO}_3^-$ and $\delta^{18}\text{O-NO}_3^-$ variables showed the influence of biogeochemical

processes that altered the initial signal. For example, the very high $\delta^{15}\text{N-NO}_3^-:\delta^{18}\text{O-NO}_3^-$ ratios (~ 1.0) during the growing season were attributable to assimilation processes, namely the uptake of NO_3^- by aquatic organisms, and less to DNRA and anaerobic ammonium oxidation (anammox), given the latter are mostly linked to estuarial settings [20]. However, the F3 site receives a considerable proportion of groundwater from Alpine karst area, so the possibility of influence from old denitrified waters cannot be fully discounted [36,38]. The FR2 site lies after the confluence with a river tributary (FR3 site), which means that the increasing and decreasing trends for $\delta^{15}\text{N-NO}_3^-$ and NO_3^- concentration values, respectively, compared to FS and FR1 sites were partly attributed to mixing with this tributary. The FR4 site showed higher $\delta^{15}\text{N-NO}_3^-$ and NO_3^- concentration values and higher compared to the FR2 site, which was attributed to increased influence of nitrate sources with higher isotope values (e.g. organic pollution); however, the concentration of NO_3^- -N remained lower compared to FS site due to mixing. The high $\delta^{15}\text{N-NO}_3^-$ values of July and August at the FR4 site coincided with low discharge and total N loading values, which were attributed to enhanced assimilation and/or denitrification signal under baseflow conditions (as evidenced by high EC values), but the signal was dampened in the Danube River, due to mixing with less NO_3^- -contaminated water. The highest $\delta^{15}\text{N-NO}_3^-$ values of December coincided with low discharge and total N loading values, which could be attributed to release of denitrified groundwater due to low precipitation amount recorded.

5. Conclusions

In summary, stable NO_3^- -N concentrations in Fischach-Dagnitz spring waters and streams are associated with highly variable $\delta^{15}\text{N}$ and $\delta^{18}\text{O-NO}_3^-$ values throughout the year. Although the long-term application of fertilizers in the catchment is the predominant source of nitrate in the spring waters, the $\delta^{15}\text{N}$ and $\delta^{18}\text{O-NO}_3^-$ values shifted towards much higher values due to denitrification, as confirmed by the $\delta^{15}\text{N-NO}_3^-$ versus NO_3^- relationship. However, $\delta^{15}\text{N-NO}_3^-:\delta^{18}\text{O-NO}_3^-$ ratios in the spring waters showed higher slopes (> 1.0) than a denitrification line, revealing the release of older denitrified water from the springs during low flow conditions. An isotope mixing model showed denitrified waters are contributing during baseflow conditions, providing $\sim 53\%$ during summer and $\sim 7\%$ during winter to the spring discharge and gaining streams. The $\delta^{15}\text{N-NO}_3^-:\delta^{18}\text{O-NO}_3^-$ ratio of ~ 1 downstream of the springs was attributed to microbial assimilation of NO_3^- during the growing season and responsible for higher $\delta^{15}\text{N}$ and $\delta^{18}\text{O-NO}_3^-$ and lower NO_3^- values observed in the gaining streams towards the confluence with the Danube River. Our study showed that nitrate isotopes can reveal 'hidden' biogeochemical and mixing processes that cannot be easily distinguished using chemical indicators and suggests the use of nitrate isotopes coupled with groundwater dating tools to provide another means to discriminate old groundwater components in gaining streams.

Acknowledgements

We acknowledge MA31 Wiener Wasser for providing discharge data at Fischach monitoring site and we thank Heike Briellmann for support. We also thank the anonymous reviewers for their comments that helped us improve the manuscript.

Disclosure statement

No potential conflict of interest was reported by the author(s).

Funding

The authors reported there is no funding associated with the work featured in this article.

Authors' contributions

I.M. and L.A. conceived the study, performed data interpretation, and wrote the manuscript; L.I.W. and M.K. performed data interpretation and revised the manuscript; L.R.M. performed data compilation and revised the manuscript; A.H. conducted geospatial data analysis and visualization and revised the manuscript; C.D. conducted the nitrate isotope analysis.

ORCID

Luis Araguás-Araguás  <http://orcid.org/0000-0001-7495-5350>

Leonard I. Wassenaar  <http://orcid.org/0000-0001-5532-0771>

Lucilena Rebelo Monteiro  <http://orcid.org/0000-0002-4457-4925>

References

- [1] Galloway JN, Dentener FJ, Capone DG, et al. Nitrogen cycles: past, present, and future. *Biogeochemistry*. 2004;70:153–226.
- [2] Matiatos I, Paraskevopoulou V, Lazogiannis K, et al. Surface–ground water interactions and hydrogeochemical evolution in a fluvio-deltaic setting: The case study of the Pinios River delta. *J Hydrol*. 2018;561:236–249.
- [3] Matiatos I, Wassenaar LI, Monteiro LR, et al. Isotopic composition ($\delta^{15}\text{N}$, $\delta^{18}\text{O}$) of nitrate in high-frequency precipitation events differentiate atmospheric processes and anthropogenic NO_x emissions. *Atmos Res*. 2022;267:105971.
- [4] Mclsaac GF, David MB, Gertner GZ, et al. Nitrate flux in the Mississippi River. *Nature*. 2001;414:166–167.
- [5] Cuello C, Correa P, Haenszel W, et al. Cancer risk and suspect environmental agents. *J Natl Cancer Inst*. 1976;57:1015–1020.
- [6] WHO. Guidelines for drinking-water quality. Vienna: World Health Organization; 2004.
- [7] Rivett MO, Buss SR, Morgan P, et al. Nitrate attenuation in groundwater: a review of biogeochemical controlling processes. *Water Res*. 2008;42:4215–4232.
- [8] Edmunds W, Bath A, Miles D. Hydrochemical evolution of the East Midlands Triassic sandstone aquifer: England. *Geochim Cosmochim Acta*. 1982;46:2069–2081.
- [9] Korom SF. Natural denitrification in the saturated zone: a review. *Water Resour Res*. 1992;28:1657–1668.
- [10] Clague J, Stenger R, Morgenstern U. The influence of unsaturated zone drainage status on denitrification and the redox succession in shallow groundwater. *Sci Total Environ*. 2019;660:1232–1244.
- [11] Cannavo P, Richaume A, Lafolie F. Fate of nitrogen and carbon in the vadose zone: in situ and laboratory measurements of seasonal variations in aerobic respiratory and denitrifying activities. *Soil Biol Biochem*. 2004;36:463–478.
- [12] Gillham R, Cherry J. Field evidence of denitrification in shallow groundwater flow systems. *Water Qual Res J*. 1978;13:53–72.

- [13] McMahon P, Böhlke J. Denitrification and mixing in a stream—aquifer system: effects on nitrate loading to surface water. *J Hydrol.* 1996;186:105–128.
- [14] Robertson W, Russell B, Cherry J. Attenuation of nitrate in aquitard sediments of southern Ontario. *J Hydrol.* 1996;180:267–281.
- [15] Suchy M, Wassenaar LI, Graham G, et al. High-frequency NO₃⁻ isotope ($\delta^{15}\text{N}$, $\delta^{18}\text{O}$) patterns in groundwater recharge reveal that short-term changes in land use and precipitation influence nitrate contamination trends. *Hydrol Earth Syst Sci.* 2018;22:4267–4279.
- [16] Wang L, Butcher AS, Stuart ME, et al. The nitrate time bomb: a numerical way to investigate nitrate storage and lag time in the unsaturated zone. *Environ Geochem Health.* 2013;35:667–681.
- [17] De Brabandere L, Brion N, Elskens M, et al. $\Delta^{15}\text{n}$ dynamics of ammonium and particulate nitrogen in a temperate eutrophic estuary. *Biogeochemistry.* 2007;82:1–14.
- [18] Derse E, Knee KL, Wankel SD, et al. Identifying sources of nitrogen to Hanalei Bay, Kauai, utilizing the nitrogen isotope signature of macroalgae. *Environ Sci Technol.* 2007;41:5217–5223.
- [19] Einsiedl F, Mayer B. Hydrodynamic and microbial processes controlling nitrate in a fissured-porous karst aquifer of the Franconian Alb.; southern Germany. *Environ Sci Technol.* 2006;40:6697–6702.
- [20] Kendall C. Isotope tracers in catchment hydrology. Amsterdam: Elsevier; 1998. Chapter 16, Tracing nitrogen sources and cycling in catchments; p. 519–576.
- [21] Luu TNM, Do TN, Matiatos I, et al. Stable isotopes as an effective tool for N nutrient source identification in a heavily urbanized and agriculturally intensive tropical lowland basin. *Biogeochemistry.* 2020;149:17–35.
- [22] Matiatos I. Nitrate source identification in groundwater of multiple land-use areas by combining isotopes and multivariate statistical analysis: A case study of Asopos basin (Central Greece). *Sci Total Environ.* 2016;541:802–814.
- [23] Obeidat M, Awawdeh M, Matiatos I, et al. Identification and apportionment of nitrate sources in the phreatic aquifers in northern Jordan using a dual isotope method ($\delta^{15}\text{N}$ and $\delta^{18}\text{O}$ of NO₃⁻). *Groundw Sustain Dev.* 2021;12:100505.
- [24] Wassenaar LI. Evaluation of the origin and fate of nitrate in the Abbotsford Aquifer using the isotopes of ¹⁵N and ¹⁸O in NO₃⁻. *Appl Geochem.* 1995;10:391–405.
- [25] Kendall C, Elliott E, Wankel S. Stable isotopes in ecology and environmental science. 2nd ed. Malden (MA): Blackwell Publishing; 2007. Chapter 12, Tracing anthropogenic inputs of nitrogen to ecosystems; p. 375–449.
- [26] Amberger A, Schmidt HL. Natürliche Isotopengehalte von Nitrat als Indikatoren für dessen Herkunft. *Geochim Cosmochim Acta.* 1987;51:2699–2705.
- [27] Mayer B, Boyer EW, Goodale C, et al. Sources of nitrate in rivers draining sixteen watersheds in the northeastern US: isotopic constraints. *Biogeochemistry.* 2002;57:171–197.
- [28] van Kessel JF. Influence of denitrification in aquatic sediments on the nitrogen content of natural waters [PhD thesis]. Wageningen: Centre for Agricultural Publishing and Documentation; 1976. (Agricultural Research Reports; 858).
- [29] Wu Y, Xu L, Wang S, et al. Nitrate attenuation in low-permeability sediments based on isotopic and microbial analyses. *Sci Total Environ.* 2018;618:15–25.
- [30] Hiscock K, Iqbal T, Feast N, et al. Isotope and reactive transport modelling of denitrification in the Lincolnshire Limestone aquifer, eastern England. *Q J Eng Geol Hydrogeol.* 2011;44:93–108.
- [31] Tesoriero AJ, Puckett LJ. O₂ reduction and denitrification rates in shallow aquifers. *Water Resour Res.* 2011;47:W12522.
- [32] Böhlke JK, O’Connell ME, Prestegard KL. Ground water stratification and delivery of nitrate to an incised stream under varying flow conditions. *J Environ Qual.* 2007;36:664–680.
- [33] Weitzman JN, Brooks JR, Mayer PM, et al. Coupling the dual isotopes of water ($\delta^2\text{H}$ and $\delta^{18}\text{O}$) and nitrate ($\delta^{15}\text{N}$ and $\delta^{18}\text{O}$): a new framework for classifying current and legacy groundwater pollution. *Environ Res Lett.* 2021;16:045008.
- [34] Salcher BC, Meurers B, Smit J, et al. Strike-slip tectonics and Quaternary basin formation along the Vienna Basin fault system inferred from Bouguer gravity derivatives. *Tectonics.* 2012;31:TC3004.

- [35] Wessely G. Zur Geologie und Hydrodynamik im südlichen Wiener Becken und seiner Randzone. *Mitteilungen der Österreichischen Geologischen Gesellschaft*. 1983;76:27–68.
- [36] Kralik M. 55 years of isotope investigations to unravel the groundwater cycles in the southern Vienna basin. *International Symposium on Isotope Hydrology: Advancing the Understanding of Water Cycle Processes CN-271 2019, May 20–24, 2019, Vienna*.
- [37] Kralik M, Humer F, Heike B, et al. ISOMETH – Endbericht: Evaluierung von Isotopen- und Spurengasmethoden zur Ermittlung von Grundwasseraltern: Fischa-Dagnitz-Quelle und Wagna Lysimeter. In: Bundesministerium für Land- und Forstwirtschaft UuW, Wien, editor. <http://www.lebensministerium.at/publikationen/wasser/flieszgewaesser/-ISOMETHEndbericht.html>; 2012. p. 27.
- [38] Stolp BJ, Solomon DK, Suckow A, et al. Age dating base flow at springs and gaining streams using helium-3 and tritium: Fischa-Dagnitz system, southern Vienna Basin, Austria. *Water Resour Res*. 2010;46:W07503.
- [39] Agency UaEE. CORINE-Landbedeckung, Nomenklatur: Level 3 (28/41 Klassen in Österreich), 25 ha kleinste berücksichtigte Flächeneinheit (MMU), Lambert-Projektion, Format: ESRI Shape File, Maßstab: 1:100.000 2018 [cited 2022]. Available from: <https://www.data.gv.at/katalog/dataset/76617316-b9e6-4bcd-ba09-e328b578fed2>.
- [40] Gewässerzustandsüberwachungsverordnung. (GZÜV RotsowqBNidgFB, Section VII/ Department 1 National Water Management; Offices of Provincial Governments and the Environment Agency Austria. H2O Data Base [cited 2022]. Available from: <https://wasser.umweltbundesamt.at/h2odb/>.
- [41] APHA. APHA standard methods for the examination of water and wastewater. Standard methods for the examination of water & wastewater. Washington (DC): American Public Health Association; 2005.
- [42] Altabet MA, Wassenaar LI, Douence C, et al. A Ti(III) reduction method for one-step conversion of seawater and freshwater nitrate into N2O for stable isotopic analysis of 15N/14N, 18O/16O and 17O/16O. *Rapid Commun Mass Spectrom*. 2019;33:1227–1239.
- [43] Clark ID, Fritz P. *Environmental isotopes in hydrogeology*. Boca Raton (FL): CRC Press; 1997.
- [44] Landesamtsdirektion LNA dNL-A. Wasserstandsnachrichten und Hochwasserprognosen [Published [cited 11-02-2022]. Available from: <https://www.noel.gv.at/wasserstand/#/en/Messstellen/Map/Grundwasserspiegel>.
- [45] Böttcher J, Strebel O, Voerkelius S, et al. Using isotope fractionation of nitrate-nitrogen and nitrate-oxygen for evaluation of microbial denitrification in a sandy aquifer. *J Hydrol*. 1990;114:413–424.
- [46] Amundson R, Austin AT, Schuur EAG, et al. Global patterns of the isotopic composition of soil and plant nitrogen. *Global Biogeochem Cycl*. 2003;17:1031.
- [47] Bateman AS, Kelly SD. Fertilizer nitrogen isotope signatures. *Isot Environ Health Stud*. 2007;43:237–247.
- [48] Fogg GE, Rolston D, Decker D, et al. Spatial variation in nitrogen isotope values beneath nitrate contamination sources. *Groundwater*. 1998;36:418–426.
- [49] Venkiteswaran JJ, Wassenaar LI, Schiff SL. Dynamics of dissolved oxygen isotopic ratios: a transient model to quantify primary production: community respiration, and air–water exchange in aquatic ecosystems. *Oecologia*. 2007;153:385–398.
- [50] Venkiteswaran JJ, Boeckx P, Goody DC. Towards a global interpretation of dual nitrate isotopes in surface waters. *J Hydrol X*. 2019;4:100037.
- [51] Craig H. Isotopic variations in meteoric waters. *Science*. 1961;133:1702–1703.
- [52] Hager B, Foelsche U. Stable isotope composition of precipitation in Austria. *Austrian J Earth Sci*. 2015;108:2–14.
- [53] IAEA/WMO. Global Network of Isotopes in Precipitation. The GNIP Database. [Published 2022]. Available from: <http://www.iaea.org/water>.
- [54] Halder J, Vystavna Y, Wassenaar L. Nitrate sources and mixing in the Danube watershed: implications for transboundary river basin monitoring and management. *Sci Rep*. 2022;12:2150.
- [55] Matiatos I, Wassenaar LI, Monteiro LR, et al. Global patterns of nitrate isotope composition in rivers and adjacent aquifers reveal reactive nitrogen cascading. *Commun Earth Environ*. 2021;2:52.

- [56] Mariotti A, Germon J, Hubert P, et al. Experimental determination of nitrogen kinetic isotope fractionation: some principles; illustration for the denitrification and nitrification processes. *Plant Soil*. 1981;62:413–430.
- [57] Granger J, Wankel SD. Isotopic overprinting of nitrification on denitrification as a ubiquitous and unifying feature of environmental nitrogen cycling. *Proc Natl Acad Sci USA*. 2016;113: E6391–EE400.
- [58] Boshers DS, Granger J, Tobias CR, et al. Constraining the oxygen isotopic composition of nitrate produced by nitrification. *Environ Sci Technol*. 2019;53:1206–1216.
- [59] Fogel ML, Cifuentes LA. Isotope fractionation during primary production. In: Engel MH, Macko SA, editor. *Organic geochemistry. principles and applications*. New York: Plenum Press; 1993. p. 73–98.
- [60] Appelo CAJ, Postma D, et al. *Geochemistry, groundwater and pollution*. London: CRC Press; 2004.
- [61] Kralik M, Stewart M. Tritium concentration in the Fischa-Dagnitz Spring reinterpreted with improved lumped parameter and hydrogeological models of the Southern Vienna Basin. *Proceedings 20th EGU General Assembly: EGU2018, 4–13 April, 2018, Vienna, Austria*. p. 8936.